

1
2
3
4
5
6
7
8
9
10
11
12
13
14
15
16
17
18
19
20
21
22
23
24
25
26
27
28
29
30

Development and Validation of a MALDI-TOF-Based Model to Predict Extended Spectrum Beta-Lactamase and/or Carbapenemase-Producing in *Klebsiella pneumoniae* Clinical Isolates

Alejandro Guerrero-López (1)(2)*, Ana Candela (2), Carlos Sevilla-Salcedo (1), Marta Hernández-García (3)(4), Pablo M. Olmos (1)(2), Rafael Cantón (3)(4), Patricia Muñoz (2)(5)(6)(7), Rosa del Campo (3)(4), Vanessa Gómez-Verdejo (1), Belén Rodríguez-Sánchez (2)(5).

(1) Department of Signal Theory and Communication, University Carlos III of Madrid, Madrid, Spain.

(2) Gregorio Marañón Health Research Institute, Hospital Gregorio Marañón, Madrid, Spain.

(3) Department of Microbiology, Hospital Ramón y Cajal and Instituto Ramón y Cajal de Investigación Sanitaria (IRYCIS). Madrid, Spain.

(4) CIBER en Enfermedades Infecciosas. Madrid, Spain.

(5) Clinical Microbiology and Infectious Diseases Department, Hospital General Universitario Gregorio Marañón, Madrid, Spain

(6) CIBER de Enfermedades Respiratorias (CIBERES CB06/06/0058), Madrid, Spain

(7) Medicine Department, Faculty of Medicine, Universidad Complutense de Madrid, Madrid, Spain

***Corresponding author**

Alejandro Guerrero-López

Theory Signal Group, Dpt. of Signal Theory and Communications

Universidad Carlos III de Madrid, Office 4.3.A03

Av. de la Universidad, 30, Leganés, 28911, Madrid, Spain,

Email: alexjorguer@tsc.uc3m.es

Phone: +34 916 248 839

FILE STATEMENT:

- **ABSTRACT LENGTH:** 238 (250 max)

- **PAPER LENGTH:** 2461 (2500 max)

31 **ABSTRACT**

32 **Objectives:** MALDI-TOF Mass Spectrometry (MS) is a reference method for microbial
33 identification at clinical microbiology laboratories. We have designed and validated a new
34 multiview model based on machine learning from MS spectra to predict antibiotic resistance
35 mechanisms 24 h before phenotypic results are available.

36 **Methods:** Antibiotic susceptibility of 402 clinical *Klebsiella pneumoniae* isolates was
37 determined in two collections, discriminating among Wild Type (WT), Extended-Spectrum
38 Beta-Lactamases (ESBL) producers, and ESBL and Carbapenemases (ESBL+CP) producers.
39 Each isolate was subcultured 3 consecutive days and 2 independent spectra were acquired in
40 each replica (6 MS spectra/isolate). Spectra were automatically classified by a kernelized
41 Bayesian factor analysis model (KSSHIBA), using two independent strategies: 1) the model
42 was designed with isolates from a single centre and validated with isolates from the other
43 centre; and 2) in a second stage all isolates were used at the same time for design and validation
44 processes.

45 **Results:** Higher prediction values were obtained when integrating all isolates with hospital
46 collection of origin information. Our model exhibited higher prediction capability than current
47 state-of-the-art models, particularly in intercollection scenarios because local epidemiology
48 could introduce relevant variables affecting prediction accuracy.

49 **Conclusions:** Compared to previously reported studies, our model demonstrated the highest
50 ability to predict ESBL and/or CP production in clinical *K. pneumoniae* isolates and it provided
51 an efficient way to combine information from different centres. Its implementation in
52 microbiological laboratories could improve the detection of multi-drug resistant isolates,
53 optimizing the therapeutic decision.

54

55 INTRODUCTION

56 Multidrug-resistant *Klebsiella pneumoniae* is considered a global public health threat
57 according to the major international health organizations due to its rapid spread, its high
58 morbidity and mortality and the economic burden associated with its treatment and control [1–
59 3]. Resistance to carbapenems is a major challenge since this antibiotic group represents one
60 of the last therapeutic options. In fact, some Carbapenemases (CP) have been shown to
61 hydrolyse almost all beta-lactam antibiotics [4]. Thus, besides the routinely antimicrobial
62 susceptibility testing (AST), rapid diagnostic methods such as MALDI-TOF Mass
63 Spectrometry (MS) should be implemented in clinical microbiology laboratories beyond
64 identification for early detection of multidrug resistant isolates.

65 MALDI-TOF MS is designed for microbial identification, but also allows the detection
66 of extended-spectrum beta-lactamases (ESBL) and CP by the different molecular weight of the
67 antibiotic after its hydrolysis by resistant bacteria [5]. This approach is faster than conventional
68 AST (30-60 min vs. 18-24 h) but requires highly trained personnel and it is of limited use in
69 clinical laboratories.

70 More recently, machine-learning methods such as Support Vector Machines (SVM),
71 Random Forest (RF), K-Nearest Neighbours (KNN), naïve Bayes and Logistic Regression have
72 been successfully applied to predict CP-producing isolates from MS spectra [6]; as well as
73 other approaches based on deep learning methods [7]. Supervised learning is a powerful
74 classification tool but is not yet optimized for the usual high-dimensional MS data.
75 Consequently, pre-processing is needed to reduce dimensions; in this sense, some authors have
76 proposed the use of a genetic algorithm in combination with a SVM using ClinProTools [8].
77 Bayesian models are starting to be implemented, as they get rid of cross-validation issues at
78 the same time that can provide a probability prediction with a confidence measurement. A

79 recent study has proposed the use of an *ad-hoc* non-linear kernel followed by a Gaussian
80 Process [9].

81 To address all these aspects, we have applied a novel Bayesian model called Kernelized
82 Sparse Semi-Supervised Interbattery Bayesian Analysis (KSSHIBA) [10,11] that using the MS
83 spectra and the hospital collection of origin predicts the phenotypic/genotypic AST. As
84 phenotypic AST data reproducibility between laboratories is also an unresolved issue, we have
85 included clinical collections characterized at separate centres, representing wide lineages
86 variability from distant epidemiological environments.

87

88

89

90

91

92

93

94

95

96

97

98

99

100

101

102

103

104

105

106 MATERIAL AND METHODS

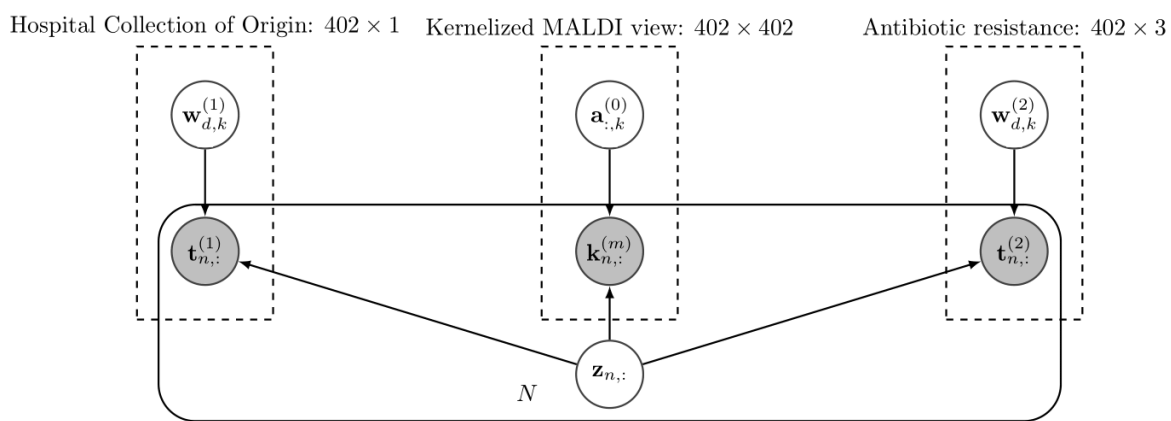
107 **Isolates selection and processing.** We included 282 consecutive clinical *K. pneumoniae*
108 isolates (2014-2019) isolated at Hospital Gregorio Marañón (GM), and 120 isolates previously
109 characterized in surveillance programs (STEP and SUPERIOR) [12,13] and sourcing from 8
110 Spanish and 11 Portuguese hospitals. This collection of isolates was merged into the Hospital
111 Ramón y Cajal collection (RyC). AST determination was performed for each collection in their
112 origin centre by the automated broth microdilution method Microscan[®] System (Beckman-
113 Coulter, CA, USA), using EUCAST criteria (2021). Presence of ESBL/CP genetic resistant
114 mechanisms was corroborated by molecular testing. Isolates were categorized as Wild Type
115 (WT) -n=94-, ESBL-producers (n=67) or ESBL+CP-producers (n=241).

116 Isolates were kept frozen at -80°C in skimmed milk and, after thawing, cultured
117 overnight at 37°C in Columbia Blood agar (bioMérieux, Lyon, France) during 3 subcultures
118 for metabolic activation. MS analysis was centralized and performed by the same operator
119 using an MBT Smart MALDI Biotyper mass spectrometer (Bruker Daltonics, Bremen), in 6
120 separated replicas (2 positions in 3 consecutive days). Protein extraction was performed adding
121 1µl 100% formic acid further dry at room temperature. Then, 1µl of HCCA matrix solution
122 (Bruker Daltonics) was added to each spot. MS spectra were acquired in the positive linear
123 mode in the range of 2,000 to 20,000 Da, using default settings [14], although only data
124 between 2,000-12,000 *m/z* was further analysed applying Total Ion Current (TIC)
125 normalization [15,16].

126

127 **Model development.** The proposed model, SSHIBA [10], considers a common low
128 dimensional latent variable, *Z*, responsible for generating heterogeneous observations of each
129 view (i.e., it can model either continuous, categorical or multilabel observations) and, besides,
130 it automatically adjusts the dimension of this latent space, finding the relationships between

131 the different views and making an interpretability analysis easier. To deal with the high
 132 dimensionality of the MS spectra data, we applied here the KSSHIBA [11] extension since it
 133 is able to model kernelized version data to work in the dual space by means of the kernel trick
 134 and avoiding the high dimensionality problem of the MS spectra. In our setting, KSSHIBA
 135 model used three complementary views: the Kernelized MS spectra, the hospital collection
 136 origin (GM or RyC), and the antibiotic resistance category (WT, ESBL and ESBL+CP) (Figure
 137 1).



139 **Figure 1.** KSSHIBA graphical model proposed integrating 3 views: kernelized MS spectra,
 140 Hospital Collection origin (GM or RyC), and antibiotic resistance category (WT, ESBL, and
 141 ESBL+CP).

142

143 **Model validation.** To test whether intra and intercollection distributions could improve the
 144 learning process, two different scenarios were proposed. First, GM and RyC collections were
 145 tested separately (intra-collection analysis), and in a second stage all isolates were merged in a
 146 single collection (inter-collection analysis).

147 In the first experiment, we split each dataset into 5 random train-validation folds. Each
 148 training fold was processed to correct the unbalance in the class population by oversampling
 149 the minority class on each antimicrobial resistance category ultimately resulting in stratified
 150 folds with a consistent class ratio. In the second experiment using the global collection, data

151 were again split into 5 random train-test folds maintaining the previous unbalance correction
152 technique. Moreover, we defined two frameworks: (1) directly combining both datasets and (2)
153 merging them with an extra view identifying as “0” isolates from GM and as “1” those from
154 RyC.

155

156 **Comparison with state-of-the-art methods.** Firstly, KSSHIBA was compared with a SVM
157 and a GP since both approaches can also work in a dual space. For these models we tried out a
158 nonlinear kernel called Radial Basis Kernel (RBF) and a linear kernel. As we were solving a
159 multidimensional problem with MS spectra and both models work for single output prediction,
160 we ran independent SVMs and GPs for each prediction task. We also compared KSSHIBA to
161 a RF able to jointly estimate all the prediction tasks. Finally, we explored our model
162 implementing the kernel called Peak Information KErnel (PIKE) [9], which exploits non-linear
163 correlations between MS peaks. In this case, MS spectra were pre-processed by a topological
164 peak selection keeping only 200 peaks per sample, as they explain in their work.

165 Hyper-parameter cross-validation was done by an inner 5-fold over the training folds.
166 We cross-validated the C value (0.01, 0.1, 1, 10) for the SVM and the number of estimators
167 (50, 100, 150) and the maximum number of features (auto, log2) for the RF. For both
168 KSSHIBA and GP, the hyper-parameters were optimized by maximizing the evidence lower
169 bound and the log marginal likelihood of the data, respectively. Then, we ran both models 5
170 times for each one to ensure that the learnt parameters do not correspond to a local maximum.
171 When KSSHIBA was combined with the PIKE kernel we fixed the kernel smoothing parameter
172 “t” to 5, based on the influence analysis carried out in the original research.

173 The extended comparison to other baselines, such as KNN, RF or SVM and GP with
174 other kernels are included in the Supplementary Material B.

175

176 **Performance metric.** Prediction of antibiotic resistance category was calculated by the AUC
177 measuring. The Receiver Operator Characteristic curve is an evaluation metric used in binary
178 classification problems that show the True Positive Rate against the False Positive Rate at
179 different thresholds. The AUC measures the ability of the model to distinguish between classes
180 (positive and negative) for different thresholds in the probability prediction and is a summary
181 of the ROC curve. Higher values of AUC means that the models distinguish better between
182 WT and non-WT isolates.

183

184 **Repository.** The model is implemented in Python using Pytorch and Pyro libraries. The code
185 used to obtain the presented results, an explanation on how to use KSSHIBA and both datasets
186 are publicly available in [17].

187

188 **Ethics Statement.** The Ethics Committee from the GM and RyC hospitals (codes
189 MICRO.HGUGM.2020-002, and 087–16, respectively) approved this study. The study was
190 performed from microbiological samples, not human products and informed consent from the
191 patients was not necessary.

192

193

194

195

196

197 RESULTS

198 A detailed description of the datasets decomposition in each scenario can be found in
 199 Supplementary Material A. The experiment's source code can be found at the GitHub
 200 repository [17].

201 Intra-collection scenario

202 Results obtained for GM and RyC separated collections are summarized in Table 1. For
 203 GM isolates, KSSHIBA performs better AUC scores than the baselines regardless of the
 204 predicted antibiotic resistance category. Specifically, nonlinear kernels provided the best
 205 results, where the RBF kernel performed better in the prediction of both ESBL and ESBL+CP
 206 and the PIKE kernel worked better for WT prediction. In the RyC collection KSSHIBA was
 207 more accurate for WT prediction while performing competitive results in ESBL prediction.

208 **Table 1.** AUC mean and standard deviation for GM and RyC intracollection analysis. The
 209 kernel type is detailed in brackets, if used, and values in bold correspond to the high prediction
 210 value for each antibiotic resistance category.

211

Dataset	Category	KSSHIBA (RBF)	KSSHIBA (LINEAR)	KSSHIBA (PIKE)	GP (LINEAR)	SVM (RBF)	RF
GM	WT	0.61±0.14	0.70±0.15	0.71±0.16	0.70±0.18	0.67±0.12	0.70±0.17
	ESBL	0.57±0.28	0.46±0.19	0.56±0.32	0.54±0.18	0.40±0.29	0.39±0.21
	ESBL+CP	0.85±0.14	0.77±0.16	0.78±0.09	0.80±0.20	0.82±0.19	0.80±0.19
RyC	WT	0.47±0.35	0.49±0.22	0.64±0.19	0.48±0.28	0.45±0.15	0.57±0.26
	ESBL	0.70±0.10	0.59±0.08	0.43±0.09	0.58±0.14	0.72±0.14	0.69±0.10
	ESBL+CP	0.67±0.12	0.66±0.05	0.43±0.09	0.62±0.06	0.71±0.17	0.71±0.07

212

213 Inter-collection scenario

214 Table 2 shows the results obtained when training simultaneously GM and RyC isolated.
 215 Labelled KSSHIBA, which means that each sample is labelled indicating from which collection
 216 is coming from, outperforms every baseline for GM isolates while also performs better for the
 217 prediction of WT and ESBL+CP isolates in RyC. The lower performance of the baselines
 218 without the source label indicates that using the data from both datasets without identifying
 219 their origin produced biased results. However, merging both collections, by adding an extra
 220 label with the collection origin, clearly contributed to improve the results in terms of AUC in
 221 all antibiotic resistance categories apart from ESBL, where there is a large imbalance (see Table
 222 S1).

223 **Table 2.** AUC mean and standard deviation when all isolates were merged in a single
 224 collection. Each model is defined with its name and the type of kernel in brackets, if used.
 225 Values in bold correspond to the high prediction for each antibiotic resistance category.
 226 Labelled means that the samples have the hospital collection origin view, whereas unlabelled
 227 means that this information is not considered by model.

Dataset	Category	KSSHIBA	KSSHIBA	GP	SVM
		(LINEAR)	(LINEAR)	(LINEAR)	(RBF)
		LABELED	UNLABELED	UNLABELED	UNLABELED
GM	WT	0.77±0.11	0.72±0.14	0.76±0.10	0.62±0.13
	ESBL	0.46±0.19	0.39±0.21	0.43±0.20	0.39±0.21
	ESBL+CP	0.88±0.08	0.86±0.10	0.86±0.08	0.85±0.08
RyC	WT	0.70±0.16	0.66±0.16	0.68±0.17	0.59±0.20
	ESBL	0.55±0.09	0.49±0.09	0.60±0.10	0.69±0.12
	ESBL+CP	0.68±0.10	0.64±0.06	0.64±0.04	0.66±0.14

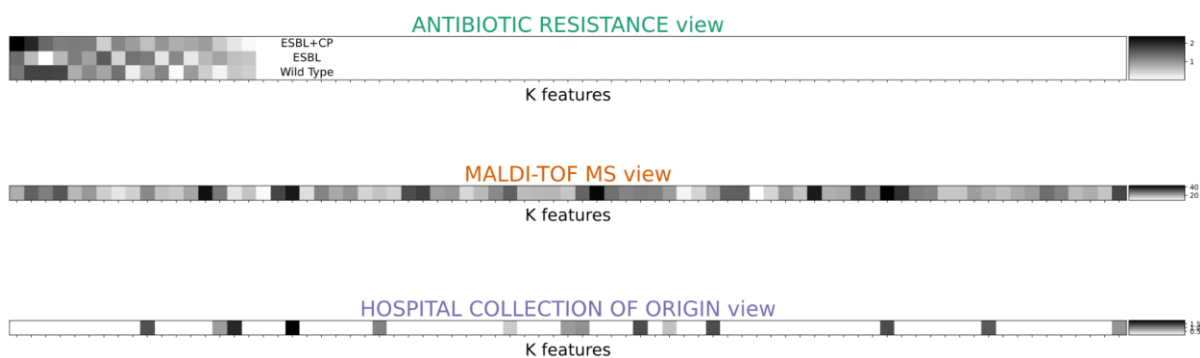
228

229 Latent space analysis of our model

230 The learnt weight matrix W of each view to evaluate the importance of each latent variable and
231 analyse how they relate to each other is shown in Figure 2; in MS view these weights are
232 averaged over the input MS dimensions to obtain an intensity value per latent factor. Here, due
233 to the sparsity imposed, the model automatically learned which latent features were relevant
234 for each view and, in turn, some of the views only used selected features.

235 KSSHIBA projected the 3 input views into 76 latent features (Figure 2), which were
236 ordered by importance in the prediction task. Noticeably, only 13 latent factors were used to
237 predict the antibiotic resistance category, all of them shared information with MS while only 3
238 of them correlated simultaneously all the information available. Finally, note 51 latent features
239 private to MS spectra view, which corresponds to an unsupervised projection of the data that
240 can be understood as a principal component analysis.

241



242

243 **Figure 2.** KSSHIBA latent space projection ($d=76$) for hospital collection origin, MS spectra,
244 and antibiotic resistance category, including data with the extra hospital collection of origin
245 view. Each subfigure refers to a W matrix associated with each view.

246

247

248 KSSHIBA showed that there existed a correlation between the hospital collection of
249 origin of each strain and their AST profile shown in the latent space that these views share.
250 This latent space representation allowed KSSHIBA to outperform all baselines in the
251 intercollection scenario. As seen in Table 2, KSSHIBA performed 0.88 ± 0.08 , 0.46 ± 0.19 and
252 0.77 ± 0.11 in GM for ESBL+CP, ESBL and WT, respectively, outperforming the state-of-the-
253 art models. Likewise, in RyC data our proposal performed better in both ESBL+CP and WT
254 prediction with AUC values of 0.68 ± 0.10 and 0.70 ± 0.16 , respectively.

255

256

257

258

259

260

261

262

263

264

265

266

267

268

269

270

271

272 DISCUSSION

273 MS allows rapid and accurate bacterial identification, and the resulting spectra can be
274 analysed by machine learning approaches to predict antibiotic resistance, as it has been
275 previously suggested [18]. The most relevant limitation for this methodology is the great
276 complexity of MS spectra, which is also influenced by the particularities of each lineage and
277 its accessory genome. In this sense, two isolates carrying the same CP gene could differ in the
278 MS spectra due to their particular genetic background. For the present work, two different
279 bacterial sets were included, one of them sourcing from the same hospital collection without
280 any particular criteria of inclusion and the other one grouped strain from 18 geographical
281 disperse hospitals selected by their phenotypic and genotypic beta-lactams resistance. The
282 latter collection was characterized by whole-genome sequencing and includes both frequent
283 and rare clonal lineages.

284 ESBL and CP categories groups a highly variable set of different proteins but with a
285 common phenotypic pattern of antibiotic susceptibility. Here, we developed and validated a
286 novel model in *K. pneumoniae* clinical isolates for ESBL and CP-producing prediction based
287 on MS spectra. Our major contribution is provided by the multiview nature of KSSHIBA since
288 it was able to learn from intercollection distribution without getting biased by intracollection
289 distributions using the hospital collection of origin as an extra view. Moreover, our model also
290 reduced the training complexity by kernel application and getting rid of cross-validation issues
291 by the optimization of the evidence lower bound exploiting the Bayesian framework. As a
292 direct consequence of these actions, the training period was considerably reduced.

293 When we used a complex (non-linear) kernel, our model got better results in
294 intracollection data: 0.85+-0.14 in ESBL+CP, 0.57+-0.28 in ESBL and 0.71+-0.16 in WT in
295 GM and 0.64+-0.19 in WT in RyC (Table 1). Although the results seemed to indicate that the
296 solution was to use complex kernels, when we combined both collections (intercollection

297 scenario, Table 2), complex kernels obtained poorer results, pointing to a possible over-fit to
298 the intracollection distributions in the first scenario. For the intracollection scenario, KSSHIBA
299 (UNLABELLED) failed to achieve better results than the baselines, but this result could be a
300 consequence of the overrepresentation of ESBL/CP in the RyC collection with respect to the
301 GM collection without inclusion criteria. This imbalance was particularly visible in the AUC
302 performance as all unlabelled models predicted ESBL significantly worse in the GM dataset
303 (unbalanced) than in the RyC dataset (balanced). Likewise, WT isolates were significantly
304 more balanced only in the GM dataset. Therefore, the unlabelled models predicted worse
305 unbalanced scenarios, getting biased by the data distribution. However, KSSHIBA
306 (LABELLED) proved that exploiting the multi-view heterogeneous features allowed to add
307 additional information to the learning process, such as the dataset source, being able to properly
308 model different data distributions getting rid of the introduced bias by the data itself. Therefore,
309 our model represents a step forward in the prediction of antibiotic resistance, particularly to
310 beta-lactam antibiotics, as it obtains better performance in terms of AUC than previous models,
311 while providing new features: adding more data to the learning base, reducing dimensionality
312 and providing interpretability of how the data sets interact with each other to predict.

313 Previous reports suggested some protein peaks are associated with specific mechanisms
314 of antibiotic resistance [19]. These observations were manually performed by direct
315 visualization of the protein spectra, but obviously automation avoids operator-related bias and
316 provides more information about the optimal areas of the spectrum for discrimination.
317 Likewise, some person-related discrepancies may occur in AST for the WT/resistant
318 categories. Although the same AST methodology was used in both collections, we cannot rule-
319 out possible discrepancies linked to each centre/person. On the contrary, a single worker in the
320 same instrument performed all MS spectra. A limitation of our work was a reduced number of
321 isolates for machine-learning methodology. Also, more geographically unrelated isolates

322 should be included, always combining the phenotypic and the genotypic previous
323 characterization of the antimicrobial susceptibility profile. Although machine-learning
324 applications on MS spectra to predict resistance to antibiotics are still in an initial stage, their
325 great potential should encourage us to continue work in this direction.

326

327 **Transparency declaration**

328

329 The authors declare that the research was conducted in the absence of any commercial or
330 financial relationships that could be construed as a potential conflict of interest.

331

332 **Funding**

333 The work of Pablo M. Olmos is supported by Spanish MINECO (Agencia Estatal de
334 Investigación) grants TEC2017-92552-EXP and RTI2018-099655-B-100; the Comunidad de
335 Madrid under grants IND2017/TIC-7618, IND2018/TIC-9649, IND2020/TIC-17372, and
336 Y2018/TCS-4705; the BBVA Foundation under the Domain Alignment and Data Wrangling
337 with Deep Generative Models (Deep-DARWiN) project; and the European Union (European
338 Regional Development Fund and the European Research Council) through the European
339 Union's Horizon 2020 Research and Innovation Program under grant 714161. C. Sevilla-
340 Salcedo, A. Guerrero-López and V. Gómez-Verdejo's are partly funded by the Spanish
341 MINECO (Agencia Estatal de Investigación) grants TEC2017-83838-R and PID2020-
342 115363RB-I00. A. Guerrero-López was also funded by the Intramural Program of the Gregorio
343 Marañón Health Research Institute. This work was supported by the projects PI15/01073 and
344 PI18/00997 from the Health Research Fund (Instituto de Salud Carlos III. Plan Nacional de
345 I+D+I 2013-2016) of the Carlos III Health Institute (ISCIII, Madrid, Spain) partially financed
346 by the European Regional Development Fund (FEDER) 'A way of making Europe'. Belén
347 Rodríguez-Sánchez is a recipient of a Miguel Servet contract (CPII19/00002) supported by the

348 Health Research Fund. The SUPERIOR Study Group includes the following members:
349 Antonio Oliver and Xavier Mulet (Hospital Universitario Son Espases, Palma de Mallorca,
350 Spain); Emilia Cercenado (Hospital General Universitario Gregorio Marañón, Madrid, Spain);
351 Germán Bou and M. Carmen Fernández (Hospital Universitario A Coruña, A Coruña, Spain);
352 Álvaro Pascual and Mercedes Delgado-Valverde (Hospital Universitario Virgen Macarena,
353 Sevilla, Spain); Concepción Gimeno and Nuria Tormo (Consortio Hospital General
354 Universitario de Valencia, Valencia, Spain); Jorge Calvo, Jesús Rodríguez-Lozano and Ana
355 Ávila Alonso (Hospital Universitario Marqués de Valdecilla, Santander, Spain); Jordi Vila,
356 Francesc Marco and Cristina Pitart (Hospital Clínic, Barcelona, Spain); and María García del
357 Castillo, Sergio García-Fernández, Marta Hernández-García, Marta Tato and Rafael Cantón
358 (Hospital Universitario Ramón y Cajal, Madrid, Spain). This study was sponsored by MSD
359 Spain. The STEP Study Group includes the following members: José Melo-Cristino (Serviço
360 de Microbiologia Centro Hospitalar Lisboa Norte, Lisboa, Portugal); Margarida F. Pinto,
361 Cristina Marcelo, Helena Peres, Isabel Lourenço, Isabel Peres, João Marques, Odete Chantre
362 and Teresa Pina (Laboratório de Microbiologia, Serviço de Patologia Clínica, Centro
363 Hospitalar Universitário Lisboa Central, Lisboa, Portugal); Elsa Gonçalves and Cristina
364 Toscano (Laboratório de Microbiologia Clínica Centro Hospitalar de Lisboa Ocidental, Lisboa,
365 Portugal); Valquíria Alves (Serviço de Microbiologia, Unidade Local de Saúde de Matosinhos,
366 Matosinhos, Portugal); Manuela Ribeiro, Eliana Costa and Ana Raquel Vieira (Serviço
367 Patologia Clínica, Centro Hospitalar Universitário São João, Porto, Portugal); Sónia Ferreira,
368 Raquel Diaz and Elmano Ramalheira (Serviço Patologia Clínica, Hospital Infante Dom Pedro,
369 Aveiro, Portugal); Sandra Schäfer, Luísa Tancredo and Luísa Sancho (Serviço de Patologia
370 Clínica, Fernando Fonseca, Amadora, Portugal); Ana Rodrigues and José Diogo (Serviço de
371 Microbiologia, Hospital Garcia de Orta, Almada, Portugal); Rui Ferreira (Serviço de Patologia
372 Clínica—Microbiologia—CHUA—Unidade de Portimão, Portugal); Helena Ramos, Tânia

373 Silva and Daniela Silva (Serviço de Microbiologia, Centro Hospitalar Universitário do Porto,
374 Porto, Portugal); Catarina Chaves, Carolina Queiroz and Altair Nabiev (Serviço de
375 Microbiologia, Centro Hospitalar Universitário de Coimbra, Coimbra, Portugal); Leonor
376 Pássaro, Laura Paixao, João Romano and Carolina Moura (MSD Portugal, Paço de Arcos,
377 Portugal).

378

379

380 REFERENCES

381 [1] Edward R. Carbapenem-resistant Enterobacteriaceae - Second update 2019:17.

382 [2] Carbapenem-resistant Enterobacteriaceae (CRE) n.d.:2.

383 [3] Tacconelli E. GLOBAL PRIORITY LIST OF ANTIBIOTIC-RESISTANT BACTERIA
384 TO GUIDE RESEARCH, DISCOVERY, AND DEVELOPMENT OF NEW
385 ANTIBIOTICS n.d.:7.

386 [4] Tacconelli E, Carrara E, Savoldi A, Harbarth S, Mendelson M, Monnet DL, et al.

387 Discovery, research, and development of new antibiotics: the WHO priority list of
388 antibiotic-resistant bacteria and tuberculosis. *Lancet Infect Dis* 2018;18:318–27.

389 [https://doi.org/10.1016/S1473-3099\(17\)30753-3](https://doi.org/10.1016/S1473-3099(17)30753-3).

390 [5] Oviaño M, Bou G. Matrix-Assisted Laser Desorption Ionization–Time of Flight Mass

391 Spectrometry for the Rapid Detection of Antimicrobial Resistance Mechanisms and

392 Beyond. *Clin Microbiol Rev* 2018;32:e00037-18. [https://doi.org/10.1128/CMR.00037-](https://doi.org/10.1128/CMR.00037-18)

393 18.

394 [6] Huang T-S, Lee SS-J, Lee C-C, Chang F-C. Detection of carbapenem-resistant

395 *Klebsiella pneumoniae* on the basis of matrix-assisted laser desorption ionization time-

396 of-flight mass spectrometry by using supervised machine learning approach. *PLoS ONE*

- 397 2020;15:e0228459. <https://doi.org/10.1371/journal.pone.0228459>.
- 398 [7] Esener N, Green MJ, Emes RD, Jowett B, Davies PL, Bradley AJ, et al. Discrimination
399 of contagious and environmental strains of *Streptococcus uberis* in dairy herds by means
400 of mass spectrometry and machine-learning. *Sci Rep* 2018;8:17517.
401 <https://doi.org/10.1038/s41598-018-35867-6>.
- 402 [8] Chen JHK, She KKK, Wong O-Y, Teng JLL, Yam W-C, Lau SKP, et al. Use of
403 MALDI Biotyper plus ClinProTools mass spectra analysis for correct identification of
404 *Streptococcus pneumoniae* and *Streptococcus mitis/oralis*. *J Clin Pathol* 2015;68:652–6.
405 <https://doi.org/10.1136/jclinpath-2014-202818>.
- 406 [9] Weis C, Horn M, Rieck B, Cuénod A, Egli A, Borgwardt K. Topological and kernel-
407 based microbial phenotype prediction from MALDI-TOF mass spectra. *Bioinformatics*
408 2020;36:i30–8. <https://doi.org/10.1093/bioinformatics/btaa429>.
- 409 [10] Sevilla-Salcedo C, Gómez-Verdejo V, Olmos P. Sparse Semi-supervised
410 Heterogeneous Interbattery Bayesian Analysis. *Pattern Recognit* 2021.
411 <https://doi.org/10.1016/j.patcog.2021.108141>.
- 412 [11] Sevilla-Salcedo C, Guerrero-López A, Olmos PM, Gómez-Verdejo V. Bayesian Sparse
413 Factor Analysis with Kernelized Observations. *ArXiv200600968 Cs Stat* 2021.
- 414 [12] Hernández-García M, García-Fernández S, García-Castillo M, Melo-Cristino J, Pinto
415 MF, Gonçalves E, et al. Confronting Ceftolozane-Tazobactam Susceptibility in
416 Multidrug-Resistant Enterobacterales Isolates and Whole-Genome Sequencing Results
417 (STEP Study). *Int J Antimicrob Agents* 2021;57:106259.
418 <https://doi.org/10.1016/j.ijantimicag.2020.106259>.
- 419 [13] Hernández-García M, García-Fernández S, García-Castillo M, Bou G, Cercenado E,
420 Delgado-Valverde M, et al. WGS characterization of MDR Enterobacterales with
421 different ceftolozane/tazobactam susceptibility profiles during the SUPERIOR

- 422 surveillance study in Spain. *JAC-Antimicrob Resist* 2020;2:dlaa084.
- 423 <https://doi.org/10.1093/jacamr/dlaa084>.
- 424 [14] Rodríguez-Sánchez B, Marín M, Sánchez-Carrillo C, Cercenado E, Ruiz A, Rodríguez-
425 Créixems M, et al. Improvement of matrix-assisted laser desorption/ionization time-of-
426 flight mass spectrometry identification of difficult-to-identify bacteria and its impact in
427 the workflow of a clinical microbiology laboratory. *Diagn Microbiol Infect Dis*
428 2014;79:1–6. <https://doi.org/10.1016/j.diagmicrobio.2014.01.021>.
- 429 [15] Zvezdanova ME, Arroyo MJ, Méndez G, Candela A, Mancera L, Rodríguez JG, et al.
430 Detection of azole resistance in *Aspergillus fumigatus* complex isolates using MALDI-
431 TOF mass spectrometry. *Clin Microbiol Infect* 2021.
432 <https://doi.org/10.1016/j.cmi.2021.06.005>.
- 433 [16] Rodrigues C, Passet V, Rakotondraso A, Brisse S. Identification of *Klebsiella*
434 *pneumoniae*, *Klebsiella quasipneumoniae*, *Klebsiella variicola* and Related Phylogroups
435 by MALDI-TOF Mass Spectrometry. *Front Microbiol* 2018;9:3000.
436 <https://doi.org/10.3389/fmicb.2018.03000>.
- 437 [17] Guerrero-López A. *Klebsiellas Pneumoniae Resistant Mechanisms and Antimicrobial*
438 *Resistance Prediction library*. 2021.
- 439 [18] Lau AF, Wang H, Weingarten RA, Drake SK, Suffredini AF, Garfield MK, et al. A
440 Rapid Matrix-Assisted Laser Desorption Ionization–Time of Flight Mass Spectrometry-
441 Based Method for Single-Plasmid Tracking in an Outbreak of Carbapenem-Resistant
442 Enterobacteriaceae. *J Clin Microbiol* 2014;52:2804–12.
443 <https://doi.org/10.1128/JCM.00694-14>.
- 444 [19] Correa-Martínez CL, Idelevich EA, Sparbier K, Kostrzewa M, Becker K. Rapid
445 Detection of Extended-Spectrum β -Lactamases (ESBL) and AmpC β -Lactamases in
446 Enterobacterales: Development of a Screening Panel Using the MALDI-TOF MS-Based

447 Direct-on-Target Microdroplet Growth Assay. *Front Microbiol* 2019;10:13.

448 <https://doi.org/10.3389/fmicb.2019.00013>.

449

450

451

452

453

454

455

456

457

458

459